



HAL
open science

Quantification of MWCNTs incorporated into PBTh matrix composite obtained by electrochemical polymerization and their effect on the conductive properties and structure

Dora Garduño-Jiménez, Alejandra Nuñez-Pineda, Melina Tapia-Tapia, Gerardo Salinas, Bernardo A. Frontana-Uribe

► To cite this version:

Dora Garduño-Jiménez, Alejandra Nuñez-Pineda, Melina Tapia-Tapia, Gerardo Salinas, Bernardo A. Frontana-Uribe. Quantification of MWCNTs incorporated into PBTh matrix composite obtained by electrochemical polymerization and their effect on the conductive properties and structure. *Synthetic Metals*, 2020, 268, pp.116491 -. 10.1016/j.synthmet.2020.116491 . hal-03491307

HAL Id: hal-03491307

<https://hal.science/hal-03491307>

Submitted on 15 Jul 2022

HAL is a multi-disciplinary open access archive for the deposit and dissemination of scientific research documents, whether they are published or not. The documents may come from teaching and research institutions in France or abroad, or from public or private research centers.

L'archive ouverte pluridisciplinaire **HAL**, est destinée au dépôt et à la diffusion de documents scientifiques de niveau recherche, publiés ou non, émanant des établissements d'enseignement et de recherche français ou étrangers, des laboratoires publics ou privés.



Distributed under a Creative Commons Attribution - NonCommercial 4.0 International License

1 Quantification of MWCNTs incorporated into PBTh matrix composite obtained by
2 electrochemical polymerization and their effect on the conductive properties and structure.

3 Dora Garduño-Jiménez,^a Alejandra Nuñez-Pineda,^a Melina Tapia-Tapia,^a Gerardo
4 Salinas,^{b*} Bernardo A. Frontana-Uribe^{a,c*}

5 ^aCentro Conjunto de Investigación en Química Sustentable UAEM-UNAM, Km 14.5 Carretera
6 Toluca-Atlacomulco, 50200, Toluca, México.

7 ^bUniversity Bordeaux, ISM, UMR 5255, Bordeaux INP Site ENSCBP, F 33607 Pessac, France.

8 ^cUniversidad Nacional Autónoma de México, Instituto de Química, Ciudad Universitaria,
9 Ciudad de México, 04510 México.

10
11 *Corresponding author contact: Gerardo.SalinasSanchez@enscbp.fr, bafrontu@unam.mx

12 Abstract

13 This paper describes the use of elemental combustion analysis for the simple quantification
14 of multiwalled carbon nanotubes (MWCNT's) inside a composite of polybithiophene
15 (PBTh) matrix obtained by electrochemical polymerization. The obtained percentage in
16 weight of MWCNT's inside PBTh composites prepared was found between 15% and 32 %
17 depending on the different electropolymerization scan rates and CNTs proportion present at
18 the polymerization solution. PBTh and PBTh/MWCNT composite properties were
19 evaluated by *in-situ* electrochemical conductance method. The presence of the MWCNT's
20 causes a decrease in the hysteresis value ($\Delta E_G \approx 100\text{mV}$), and a faster charge exchange
21 mainly in the charged-discharged transition, improving the conducting and electron transfer
22 properties. Atomic force microscopy (AFM) scanning electronic microscopy (SEM) and X-
23 ray diffraction (XRD) analysis let to distinguish unambiguously the presence of CNT's and
24 in the composite a nano fibrous structure was observed, which may explain the
25 improvement of the electrochemical properties.

26
27 Keywords: MWCNT, Polybithiophene, electrochemical polymerization, *in-situ*
28 electrochemical conductance

30 1. Introduction

31 Polybithiophene (PBTh) is one of the most interesting conducting polymers in the past
32 years due to its easy chemical and electrochemical synthesis and a good chemical and
33 electrochemical stability [1]. In order to improve the mechanical, physical and electrical
34 properties of conducting polymers, different types of composites have been synthesized by
35 incorporation of carbon nanotubes (CNT's) [2,3] Several examples of these type of
36 composites formed by the mixture of single walled carbon nanotubes (SWCNT's) [4] and
37 multiwalled carbon nanotubes (MWCNT's) [5,6] with different polythiophenes have been
38 studied in the last years. These materials present a considerable increase on the
39 electroactive area and conductivity [7,8], allowing their use for electrochemical sensing
40 [9,10], as supercapacitors [11,12] and in organic solar cells [3] Incorporation of CNT's
41 commonly occurs during the chemical [13] or electrochemical polymerization in a
42 suspension mixture formed by the monomer of interest, electrolyte (electrochemical
43 oxidation), oxidative agent (chemical oxidation) and different percentages in weight of
44 CNT's. Since the mechanical, physical and electric properties of these materials are
45 strongly linked to the amount of CNT's present inside the polymer matrix their efficient
46 quantification is needed. Most of the reports that involve conducting polymer (CP)
47 composites which incorporate CNT's (CP/CNTs) does not quantify the amount of this
48 carbon species that have been incorporated into the polymeric matrix, and limit the
49 composition description to the percentages in weight used of CP and CNT's in the
50 polymerization suspension [9,11] Commonly these works assume that the incorporation of
51 the carbon species is proportional to the quantity present during the polymerization. Other
52 studies present the mass percent of MWCNT's in a composite by dividing the total mass of

53 the composite by the mass of the MWCNT's used [14], or simply polymerizing in the same
54 conditions with and without CNT's and weighting the obtained samples [15]. Since
55 elemental combustion analysis is a simple and accurate method to verify the percentage of
56 elements present in an organic sample, some recent and scarce investigations describe its use
57 to follow the MWCNT's incorporation into the CP obtained by chemical oxidation with
58 FeCl₃ (PTh [6] and PEDOT [13]) composite matrix. As far as we know, this method has
59 not been applied to composites obtained by electrochemical polymerization, therefore, in
60 this work we present the use of elemental combustion analysis for the simple quantification
61 of MWCNT's inside PBTh matrix composites prepared at different scan rate and
62 concentration of MWCNT present in the polymerization solution. Finally, in order to
63 evaluate the properties of the PBTh/MWCNT composite obtained, *in-situ* electrochemical
64 conductance analysis and atomic force microscopy (AFM) scanning electronic microscopy
65 (SEM) and X-ray diffraction (XRD) studies were carried out. These studies demonstrate an
66 improved electrochemical response and an interesting change in the morphology of the
67 composite.

68 2. Experimental

69 2.1. Reagents

70 LiClO₄ (Aldrich, 99.9%), 2,2'-bithiophene (Aldrich, 97%), anhydrous ACN (Fermont
71 HPLC grade 99.9%) and multiwall carbon nanotubes (Sunnano®, ≥ 99%, OD, 10 ~ 35 nm;
72 L, 1~10µm) were used.

73 2.2. Electrochemical synthesis and characterization of PBTh/MWCNT composites

74 Cyclic voltammetry, for analyzing bithiophene (BTh) and the working media, was
75 performed in a classic three-electrode cell (WE: 3 mm Pt disk) containing anhydrous
76 acetonitrile (ACN, 5 mL) as solvent and LiClO₄ as supporting electrolyte (0.1 M) by means
77 of a BAS 100B potentiostat. The BTh concentration used for all experiments was 0.015 M.
78 Potentiodynamic macro-electropolymerizations were carried out using a three-electrodes
79 cell (Figure SI-1) fitted with an alumina 0.03 μm polished Pt foil (0.48 cm² of electroactive
80 area), a Pt mesh (0.6 cm²) and Ag/AgNO₃ used as working, counter and reference
81 electrodes respectively. The electropolymerizations were carried out at 25 °C and at three
82 different scan rates ($v = 0.1, 0.05$ and 0.02 V/s) under gentle constant stirring in order to
83 avoid CNT's sedimentation.

84 After the macro-electropolymerizations, the films were wash-out with HPLC grade ACN
85 peeled-off from the electrode and vacuum dried. The elemental combustion analysis of all
86 the films was carried out by using an Elementar® Vario Micro cube. Since from the
87 elemental combustion analysis the percentage of carbon (%C) and sulphur (%S) inside the
88 sample is obtained, the total mass of carbon and sulphur ($m_{T,Carbon}$ and $m_{T,sulphur}$
89 respectively) can be calculated by equation 1 and 2.

$$90 \quad \%C \left[\frac{1g_{Total}}{100\%_{Total}} \right] = m_{T,carbon} \quad (1)$$

$$91 \quad \%S \left[\frac{1g_{Total}}{100\%_{Total}} \right] = m_{T,sulphur} \quad (2)$$

92 Knowing that the only source of sulphur is the PBTh and per each mol of sulphur 4 mol of
93 carbon belongs to a thiophene molecule, the amount of carbon coming from PBTh
94 ($m_{PBTh,carbon}$) may be calculated by equation (3).

$$95 \quad m_{T,sulphur} \left[\frac{1 \text{ mol}_{sulphur}}{32.06 \text{ g}_{sulphur}} \right] \left[\frac{4 \text{ mol}_{carbon}}{1 \text{ mol}_{sulphur}} \right] \left[\frac{12.01 \text{ g}_{carbon}}{1 \text{ mol}_{carbon}} \right] = m_{PBTh,carbon} \quad (3)$$

96 If the total amount of carbon ($m_{T,carbon}$) is equal to the sum of carbon present in PBTh and
 97 MWCNT, the difference between the carbon of the PBTh and the total amount of carbon is
 98 equal to the amount of carbon coming from the MWCNT ($m_{MWCNT,carbon}$) (equation 4).

$$99 \quad m_{MWCNT,carbon} = m_{T,carbon} - m_{PBTh,carbon} \quad (4)$$

100 With this value the percentage in weight of MWCNT ($\%MWCNT_T$) inside the composite
 101 can be calculated (equation 5).

$$102 \quad \left[\frac{m_{MWCNT,carbon}}{m_{T,carbon}} \right] \times 100 = \%MWCNT_T \quad (5)$$

103 *In-situ* electrochemical-conductance measurements were carried out using a HEKA CIP 2
 104 bipotentiostat system specially built for this application. As working electrodes were used
 105 interdigital microarrange electrodes (IDMAE) of 1 cm x 0.5 cm, featuring separated Pt
 106 bands (10 μ m) deposited on it (Figure SI-2). A three-electrode electrochemical cell fitted
 107 with a Pt foil counter electrode separated 0.5 cm from the working electrode (parallel and
 108 of the same size of the working electrode), an Ag/AgNO₃ reference electrode and the
 109 IDMAE where used for the studies. A constant potential difference of 10 mV provided by
 110 one potentiostat was applied between the IDMAE branches to generate the drain current
 111 that circulates through the polymer during conductance determinations. The
 112 electropolymerizations were carried out at the same temperature mentioned previously.
 113 Conductance was calculated according to Ohm law, which is directly related with specific
 114 conductivity. Even though without an exact thickness value it is not possible to determine
 115 the polymer conductivity, conductance behavior is generally accepted to get a first indirect

116 insight of the conductivity changes with the redox change (see supporting information for
117 details) [16]. More details about this technique and examples of the use of conductance
118 measurements in conducting polymers can be found elsewhere in the literature [17].

119 For the morphology, surface and structure characterization, atomic force microscopy
120 (AFM) scanning electronic microscopy (SEM) and X-ray diffraction (XRD) experiments
121 were carried out. An atomic force microscope model MFP-3D Origin from the Asylum
122 Research brand of Oxford Instrument was used. Image acquisition was in AC Air
123 Topography mode and image processing and data acquisition was done with Igor Pro
124 6.34A software. The probes used for the analysis are AC 240-TS (70 kHz and 2 N/m),
125 reporting an average drive frequency of 74.8 kHz. The images corresponding to the PBTh
126 and MWCNT/PBTh samples were obtained directly on the Pt foil covered with the
127 material, scanning with a drive amplitude value of 0.240, 1.03, 0.996 V, a scan rate of 0.30,
128 0.18 and 0.22 Hz respectively and a final image of 416 points and lines in all cases. SEM
129 experiments were carried out using a Hitachi TM-1000 tabletop microscope. Powder
130 Diffractometer Bruker D8 Advance using $\text{CuK}\alpha$ radiation and equipped with a Linxeye
131 detector was used.

132 3. Results and discussion

133 The cyclic voltammetry of BTh (Figure SI-3) and the experiments in the presence of
134 different concentrations of MWCNT (Figure SI-4) using an inversion potential (E_i) at the
135 peak potential of the monomer oxidation (1.20 V vs Ag/AgNO_3) present an irreversible
136 oxidation process on the surface of the Pt electrode in the $\text{ACN}/\text{LiClO}_4$ system, showing in
137 the first reverse cycle of the voltammogram the typical trace-crossing effect observed

138 during the electrochemical polymerization of π -conjugated systems [18]. This monomer
139 oxidation process generates a PBTh/MWCNT composite [19]. A current increase of the
140 anodic and cathodic signals, which is characteristic of the growth of this type of polymers,
141 was observed (Figure 1). During the potentiodynamic macro BTh polymerization in the
142 presence of the different amount of MWCNT it was observed a higher current (ca. two -
143 three times) in the associated voltammetric curves, which is indicative of its incorporation
144 into the PBTh matrix (Figure SI-4). Similar changes have been reported for PPy-MWCNT
145 composites growth electrochemically [20]. The current observed in the cyclic voltammetry
146 curves of BTh in the presence of different amounts of MWCNT, seems at first sight to
147 show some indications of current increase with the MWCNT content, but unfortunately not
148 logical trend of this tendency was possible to confirm. A large dispersity of current values
149 was observed during the electrodeposition experiments carried out to construct table 1.
150 Consequently, figure SI-4 shows only examples of this curves. Macro-
151 electropolymerization of BTh and the composites were performed by cyclic voltammetry
152 ($Q_{a,Total} = 100$ mC), sweeping between -0.40 V and 1.2 V vs Ag/AgNO₃ and 1.25 V vs
153 Ag/AgNO₃ respectively at different scan rates (Figure 1). No change on the oxidation onset
154 potential of the charge/discharge process in the presence of the MWCNT at different scan
155 rates was observed.

156 Figure 1 here

157 The weight percentage of MWCNT's inside the different PBTh composites was obtained
158 from the macro-electropolymerizations films using equations 1-5 at different concentrations
159 of MWCNT's and scan rates (Table I). As it can be seen from these results the highest
160 weight percentage of MWCNT's was obtained at low scan rates values. Since, during the

161 macro-electropolymerization, MWCNT's are attracted to the charged oligomers of
162 bithiophene, low scan rates values allow a longer residence time in potentials where these
163 oligomers are in an oxidized state, therefore, the amount of MWCNT's inside the PBTh
164 matrix increase. The amount of MWCNT's in suspension does not influence in an
165 important way in the weight percentage of MWCNT inside the PBTh matrix. This
166 observation is important because reports sometimes assume that the quantity of carbon
167 species inside of the matrix, could be related with the material added to the polymerization
168 solution and this is not the reality as shows the present study. Since the amount of
169 MWCNT's that PBTh can insert in the matrix strongly depends on the polymerization
170 kinetics and this depends on the scan rate and temperature, thus at constant scan rate and
171 temperature the incorporated material is almost the same. However higher concentration of
172 MWCNT's in suspension, improves the reproducibility of the experiment. This probably
173 indicates that the interface concentration tends to be constant all along the experiment
174 because polymerization is carried out under gentle stirring. By this method a real
175 evaluation of the quantity of MWCNT's inside of the PBTh matrix was obtained, in
176 comparison with other studies where only the amount of NT's in suspension is indicated
177 [6,9,11]. The amount found to be incorporated agrees with the weight percentage found in
178 other CP/CNTs (PEDOT) composites, value that oscillates between 19-43% depending on
179 the experimental conditions used, determined by a similar method [13]. From this literature
180 antecedent where PEDOT was used, seems that CNTs incorporation might be controlled by
181 the polymer backbone structure (thiophenes in both cases). In this moment of our study the
182 real answer is not clear. Properties of the composite materials, CP/carbon species, strongly
183 depend on the quantity of carbon species incorporated into the polymeric matrix. Therefore,

184 this method could help to determine precisely the quantity of material that modulates the
185 desired properties for example electrochemical conductivities.

186 Table I here

187 In order to verify this proposal, *in-situ* electrochemical-conductance measurements were
188 performed (Figure 2) during the potentiodynamic electropolymerization of both, BTh and
189 BTh/MWCNT's. From the current values obtained in all our samples we can propose that
190 the thickness of the polymerizations of BTh without and with MWCNT are in the same
191 order of magnitude. If this characteristic is fulfilled, then makes sense to propose that
192 conductance value gives information of the specific conductivity behavior of the composite
193 films. These studies showed the classical current increase of the anodic and cathodic signals
194 and interestingly almost no difference was observed in the presence of the carbon species in
195 the cyclic voltammetry behavior. On the other hand, conductance response showed fast
196 electropolymerization kinetics for both experiments where the maximal conductance value
197 is higher in the presence of the CNT's (47 mS for PBTh and *ca.* 63 mS for the
198 PBTh/MWCNT's composite). The maximal value showed that the incorporation of the
199 CNT's into the PBTh matrix increases the electrical performance; therefore, electrical
200 transport in the composite is facilitated with the presence of the MWCNT's as has been
201 previously reported [6,7,8]. The conductance curve tailing observed at the end of the
202 conducting to isolating state transition, can be related to the kinetics evolution between both
203 states. In the case of PBTh, tailing is long and ends at -0.70 V vs Ag/AgNO₃, whereas the
204 PBTh/MWCNT's composite shows a shorter tailing that ends at -0.25 V vs Ag/AgNO₃.
205 This behavior let to propose that the presence of the CNT's increases the kinetics of the
206 charge/discharge process. A second argument that reinforces this statement is the

207 observation that as the scans evolve, an increase of the hysteresis value (ΔE_G) can be
208 observed for both films. The hysteresis value for the charge-discharge conductance curve
209 (ΔE_G) can be used to characterize the easiness of switching between the insulating-
210 conducting states giving also indirectly information about the internal organization of the
211 polymer matrix [21]. In the presence of the MWCNT's ΔE_G decreases *ca.* 100 mV
212 compared to the observed with PBTh showing that the transition between the conductive
213 thin film region and insulating regions is faster and less energetically demanding when
214 MWCNT's are present in the polymeric matrix. Therefore, an improvement in the transition
215 between the insulating-conducting states is confirmed and is caused by a better internal
216 organization of the polymer matrix and higher conductivity of the composite. These two
217 phenomena can be attributed to the additional possibility of extracting charged species that
218 the presence of the incorporated material causes (Figure 2) [19].

219 Figure 2 here

220 The presence of carbon nanotubes inside the PBTh matrix was verified by SEM, AFM and
221 XRD experiments. The morphology of PBTh present a granular shape, whereas the
222 PBTh/MWCNT's composite shown a more typical nano fibrous morphology (Figure SI-5).
223 This is attributed to a templating growth of the polybithiophene coating the MWCNT's
224 surface. AFM experiments show, in the case of the polymer deposit (Figure 3a) a surface
225 with globular structures with sizes of 833.24 nm in length and a Z value of 0.8 μm is
226 observed. These structures are superimposed and at the same time present ultra-structure,
227 causing that their percentage of surface is higher (44.25%) than in the case of the
228 MWCNT's coated with the polymer (10.35%, Figure 3b). The ultrastructure of PBTh has
229 an RMS value ranging from 774.562 to 966.183 nm (average value 870.3 nm), considering

230 an area of $1 \mu\text{m}^2$. In the case of the composite material, the incorporation of the NT was
231 verified by phase analysis images (Figure SI-6), since the NT coated with the polymer have
232 an increase in density, this analysis let to distinguish unambiguously from the rest of the
233 CNT's-free polymeric material. This composite material follows the longitudinal structure
234 of the MWCNT (Figure 3b), which allowed the measurement of roughness (RMS) and the
235 generation of a topographic profile (Figure SI-6a). The amplitude and phase analysis
236 (Figure SI-6b and c, respectively) shows the typical granular growth of polybithiophene
237 whose width corresponds to a polymer coating of *ca.* 250 nm towards both sides in the
238 thickest part. The CNT's covering is similar to a core-shell structure described previously
239 when the chemical oxidation (FeCl_3) of thiophene is carried out in the presence of sodium
240 bis(2-ethylhexyl) sulfosuccinate [6]. The micrograph also shows an interesting variation of
241 the polythiophene surface, clearly identified by the phase analysis of the deposited material.
242 Finally, XRD analysis of the PBTh/MWCNT's composite shows two characteristic broad
243 diffraction peaks centered at $2\theta = 17.7^\circ$ and 26° indicating the presence of PBTh and
244 CNT's in the composite matrix (Figure SI-7) [22,23]. In fact, it has been described [6] that
245 the characteristic broad peak observed in powder XRD at 2θ values ranging between 12°
246 and 25° with its maximum is centered at 18.23° attributed to the amorphous domains of the
247 PBTh chains obtained by chemical oxidation, disappears when polymerization is carried
248 out in the presence of MWCNT's and a new sharp peak observed at a 2θ value of 26.48° is
249 observed in the composite material. We agree with the authors of this work, were their
250 proposal for rationalize this observation is that aromatic rings of carbon nanotubes and
251 polythiophene would have undergone good solid-state ordering via π - π packing, that would
252 let to explain the templating growth of the polybithiophene. This nano fibrous structure also
253 explains the better conductivity and fast transition between the isolating and conducting

254 states previously described and also attributed to a better arrangement of the composite
255 macrostructure.

256 Figure 3 here

257 4. Conclusions

258 Elemental combustion analysis is presented as a simple and efficient method for the
259 quantification of multiwalled carbon nanotubes (MWCNT's) inside of macro-
260 electropolymerized conducting polymers such as PBTh. The obtained percentage in weight
261 of MWCNT's inside the PBTh composites was found between 15% and 32 %, such values
262 are in agreement with the ones reported for other CP/CNTs composites obtained chemically
263 [13]. Low scan rates allow a longer residence time in potentials where the oligomers are in
264 an oxidized state, this causes an increase in the amount of MWCNT's inside the PBTh
265 matrix. Although high concentration of MWCNT's in suspension improves the
266 reproducibility of the experiments, it does not influence in the weight percentage of
267 MWCNT inside the PBTh matrix. Incorporation of CNT's into the PBTh matrix causes an
268 improvement in the electrical transport of the composite, due to an increase of the maximal
269 conductance value (47 mS for PBTh and *ca.* 63 mS for the PBTh/MWCNT's composite).
270 In addition, an improvement in the transition between the insulating-conducting states due
271 to a better internal organization of the polymer matrix was observed. SEM, AFM and XRD
272 analysis let to distinguish unambiguously the presence of CNT's in the PBTh composite. A
273 granular growth of polybithiophene covering along the CNT's structure was observed. This
274 nano fibrous structure allows to explain the improvement on the conductivity and the fast

275 transition between the isolating and conducting states observed for the PBTh/MWCNT
276 composite.

277 5. Acknowledgements

278 The authors are grateful to PAPIIT DGAPA-UNAM Project IN208919. Ing. Citlalit
279 Martinez (CCIQS UAEMéx-UNAM), Dr. Uvaldo Hernandez Balderas and Angel Ivan
280 Torres-Pichardo are acknowledged for technical support.

281

282 6. References

- 283 [1] R. D. McCullough, The chemistry of conducting polythiophenes, *Adv. Mater.*, 10,
284 (1998), 93-116. DOI: 10.1002/(SICI)1521-4095(199801)10:2<93::AID-
285 ADMA93>3.0.CO;2-F
- 286 [2] C. Zanardi, F. Terzi, R. Seeber, Polythiophenes and polythiophene-based composites in
287 amperometric sensing, *Anal. Bioanal. Chem.*, 405, (2013), 509–531. DOI: 10.1007/s00216-
288 012-6318-7
- 289 [3] G. Keru, P. G. Ndungu, V. O. Nyamori, A review on carbon nanotube/polymer
290 composites for organic solar cells, *Int. J. Energy Res.* 38, (2014), 1635–1653. DOI:
291 10.1002/er.3194
- 292 [4] N. Terasawa, K. Asaka, High-performance PEDOT:PSS/Single-walled carbon
293 nanotube/ionic liquid actuators combining electrostatic double-layer and faradaic
294 capacitors, *Langmuir*, 32, (2016), 7210–7218. DOI: 10.1021/acs.langmuir.6b01148
- 295 [5] D. Wang, C. Lu, J. Zhao, S. Han, M. Wu, W. Chen, High energy conversion efficiency
296 conducting polymer actuators based on PEDOT:PSS/MWCNTs composite electrode, *RSC*
297 *Adv.*, 7, (2017), 31264–31271. DOI: 10.1039/c7ra05469f
- 298 [6] T. S. Swathy, M. A. Jose, M. J. Antony, AOT assisted preparation of ordered,
299 conducting and dispersible core-shell nanostructured polythiophene-MWCNT
300 nanocomposites, *Polymer*, 103, (2016), 206-213. DOI: 10.1016/j.polymer.2016.09.047

301 [7] Y. Y. Wang, K. F. Cai, S. Shen, X. Yao, In-situ fabrication and enhanced thermoelectric
302 properties of carbon nanotubes filled poly(3,4-ethylenedioxythiophene) composites, *Synth.*
303 *Met.* 209, (2015), 480-483. DOI: 10.1016/j.synthmet.2015.08.034

304 [8] J. Wang, K. Cai, J. Yin, S. Shen, Thermoelectric properties of the PEDOT/SWCNT
305 composite films prepared by a vapor phase polymerization, *Synth. Met.* 224, (2017), 27-32.
306 DOI: 10.1016/j.synthmet.2016.11.031

307 [9] M. Braik, M. M. Barsan, C. Dridi, M. B. Ali, C. M. A. Brett, Highly sensitive
308 amperometric enzyme biosensor for detection of superoxide based on conducting
309 polymer/CNT modified electrodes and superoxide dismutase, *Sensors and Actuators B*,
310 236, (2016), 574–582. DOI: 10.1016/j.snb.2016.06.032

311 [10] Z. Amirzadeh, S. Javadpour, M. Hossein-Shariat, R. Knibbe, Non-enzymatic glucose
312 sensor based on copper oxide and multi-wall carbon nanotubes using PEDOT:PSS matrix,
313 *Synth. Met.* 245, (2018), 160-166. DOI: 10.1016/j.synthmet.2018.08.021

314 [11] X. Wang, C. Yang, J. Jin, X. Li, Q. Cheng, G. Wang, High-performance stretchable
315 supercapacitors based on intrinsically stretchable acrylate rubber/MWCNTs@conductive
316 polymer composite electrodes, *J. Mater. Chem. A*, 6, (2018), 4432-4442. DOI:
317 10.1039/c7ta11173h

318 [12] D. Zhao, Q. Zhang, W. Chen, X. Yi, S. Liu, Q. Wang, Y. Liu, J. Li, X. Li, H. Yu,
319 Highly flexible and conductive cellulose-mediated PEDOT:PSS/MWCNT composite films
320 for supercapacitor electrodes, *ACS Appl. Mater. Interfaces*, 9, (2017), 13213–13222. DOI:
321 10.1021/acsami.7b01852

- 322 [13] A. Dettlaff, P. R. Das, L. Komsijska, O. Osters, J. Łuczak, M. Wilamowska-
323 Zawłocka, Electrode materials for electrochemical capacitors based on poly(3,4
324 ethylenedioxythiophene) and functionalized multi-walled carbon nanotubes characterized
325 in aqueous and aprotic electrolytes, *Synth. Met.* 244, (2018), 80-91. DOI:
326 10.1016/j.synthmet.2018.07.006
- 327 [14] H. Song, K. Cali, J. Wang, S. Shen, Influence of polymerization method on the
328 thermoelectric properties of multi-walled carbon nanotubes/polypyrrole composites, *Synth.*
329 *Met.* 211 (2016), 58–65. DOI: 10.1016/j.synthmet.2015.11.013
- 330 [15] X. Bai, X. Hu, S. Zhou, J. Yan, C. Sun, P. Chen, L. Li, In situ polymerization and
331 characterization of grafted poly (3,4-ethylenedioxythiophene)/multiwalled carbon
332 nanotubes composite with high electrochemical performances, *Electrochim. Acta*, 87,
333 (2013), 394-400. DOI: 10.1016/j.electacta.2012.09.079
- 334 [16] G. Salinas, J. A. Del-Oso, P. J. Espinoza-Montero, J. Heinze, B. A. Frontana-Urbe,
335 Electrochemical polymerization, characterization and in-situ conductivity studies of poly-
336 3,4-ortho-xylendioxythiophene (PXDOT), *Synth. Met.* 245, (2018), 135-143. DOI:
337 10.1016/j.synthmet.2018.08.020
- 338 [17] G. Salinas, B. A. Frontana-Urbe, Analysis of conjugated polymers conductivity by in
339 situ electrochemical-conductance method, *ChemElectroChem*, 6, (2019), 4105-4117. DOI:
340 10.1002/celec.201801488

- 341 [18] J. Heinze, A. Rasche, M. Pagels, B. Geschke, On the origin of the so-called nucleation
342 loop during electropolymerization of conducting polymers, *J. Phys. Chem. B*, 111 (2007)
343 989–997. DOI: 10.1021/jp066413p
- 344 [19] A. G. Porras-Gutiérrez, B. A. Frontana-Uribe, S. Gutiérrez-Granados, S. Griveau, F.
345 Bedioui, In situ characterization by cyclic voltammetry and conductance of composites
346 based on polypyrrole, multi-walled carbon nanotubes and cobalt phthalocyanine,
347 *Electrochim. Acta*, 89, (2013), 840– 847. DOI: 10.1016/j.electacta.2012.11.018
- 348 [20] M. Hughes, G. Z. Chen, M. S. P Shaffer, D. J. Fray, A. H. Windle, Electrochemical
349 Capacitance of a Nanoporous Composite of Carbon Nanotubes and Polypyrrole, *Chem.*
350 *Mater.*, 14, (2002), 1610-1613
- 351 [21] K. M. Nalin de Silva, E. Hwang, W. K. Serem, F. R. Fronczek, J. C. Garno, E. E.
352 Nesterov, Long-chain 3,4-ethylenedioxythiophene/thiophene oligomers and
353 semiconducting thin films prepared by their electropolymerization, *ACS Appl. Mater.*
354 *Interfaces*, 4, (2012), 5430-5441. DOI: 10.1021/am301349g
- 355 [22] T. Sato, M. Fujitsuka, H. Segawa, T. Shimidzu, K. Tanaka, Dual Photoluminescence
356 of polythiophenes thin films, *Synth. Met.* 95, (1998), 107-112. DOI: 10.1016/S0379-
357 6779(98)00040-X
- 358 [23] L. Wang, X. Jia, D. Wang, G. Zhu, J. Li, Preparation and thermoelectric properties of
359 polythiophene/multiwalled carbon nanotube composites, *Synth. Met.* 181 (2013) 79–85.
360 DOI: 10.1016/j.synthmet.2013.08.011

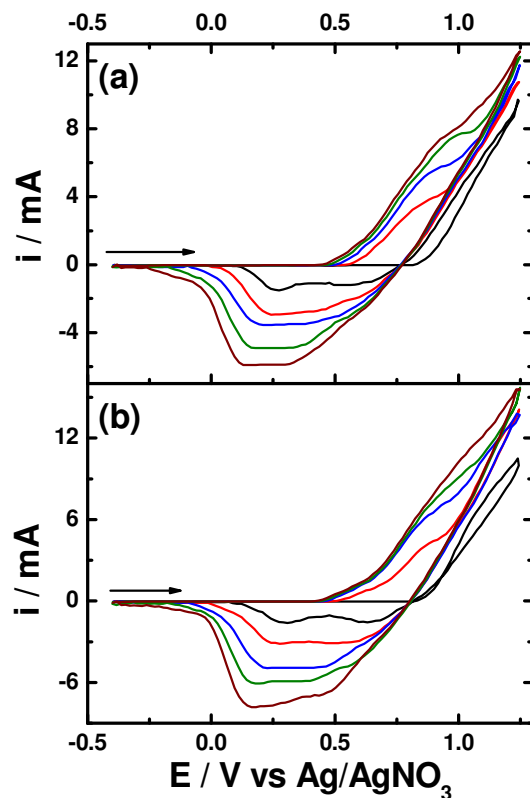
361

362 Table 1. Percentage weight of MWCNT's incorporated in PBTh matrix composites
363 obtained by elemental combustion analysis, for different scan rates and mass content of
364 MWCNT in the electropolymerization suspension. The results shown are the average of
365 three independent experiments.

<i>Scan rate</i>	<i>MWCNT's</i>		
	<i>10 mg</i>	<i>20 mg</i>	<i>40 mg</i>
<i>0.02 V/s</i>	27.66 % ± 5.07	28.25 % ± 5.54	31.48 % ± 0.56
<i>0.05 V/s</i>	19.17 % ± 4.63	21.34 % ± 0.03	21.58 % ± 1.63
<i>0.1 V/s</i>	15.53 % ± 1.91	15.16 % ± 3.87	16.59 % ± 1.39

366

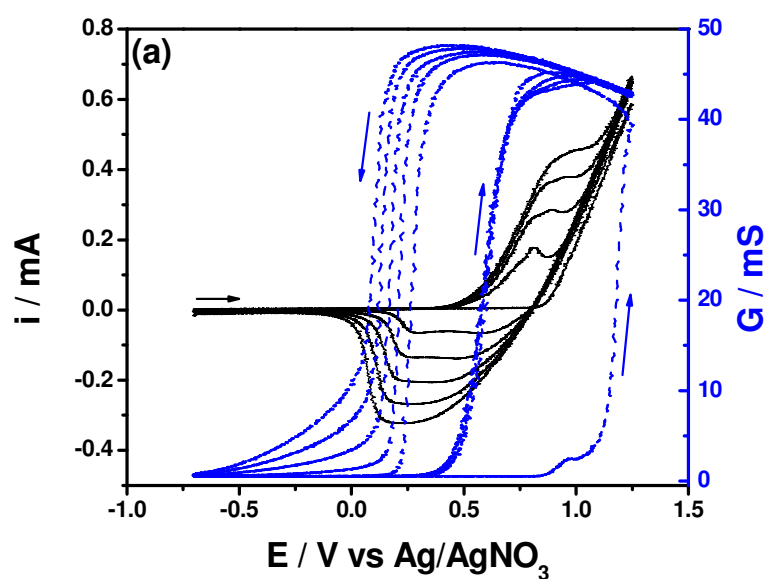
367



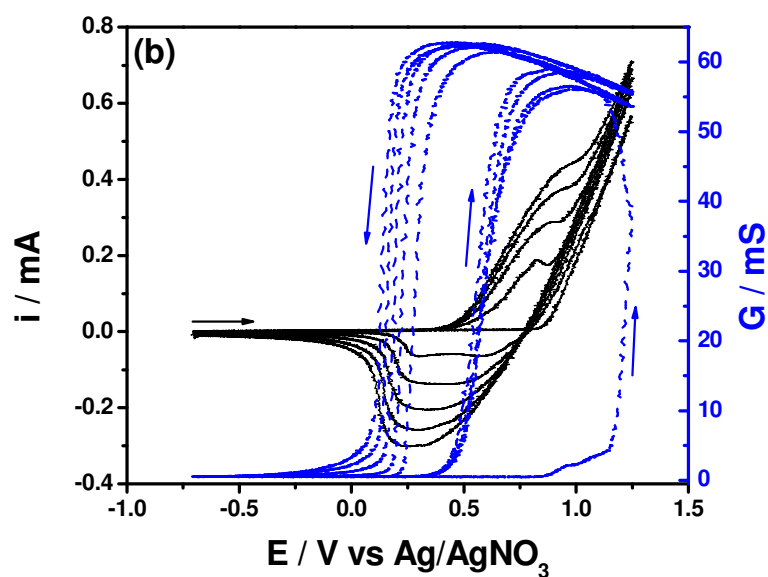
368

369 Figure 1. Macro-electropolymerization of BTh/MWCNT mixture in a ACN/LiClO₄ 0.1 M,
 370 0.015 M BTh, 40 mg MWCNT solution under constant stirring, $T = 25^{\circ}\text{C}$, WE=Pt sheet
 371 (0.48 cm²), CE=Pt foil (0.6 cm²), $E_i = -0.40\text{ V vs Ag/AgNO}_3$, $E_\lambda = 1.20\text{ V vs Ag/AgNO}_3$, 5
 372 cycles, (a) $\nu = 0.02\text{ V s}^{-1}$ and (b) $\nu = 0.1\text{ V s}^{-1}$.

373

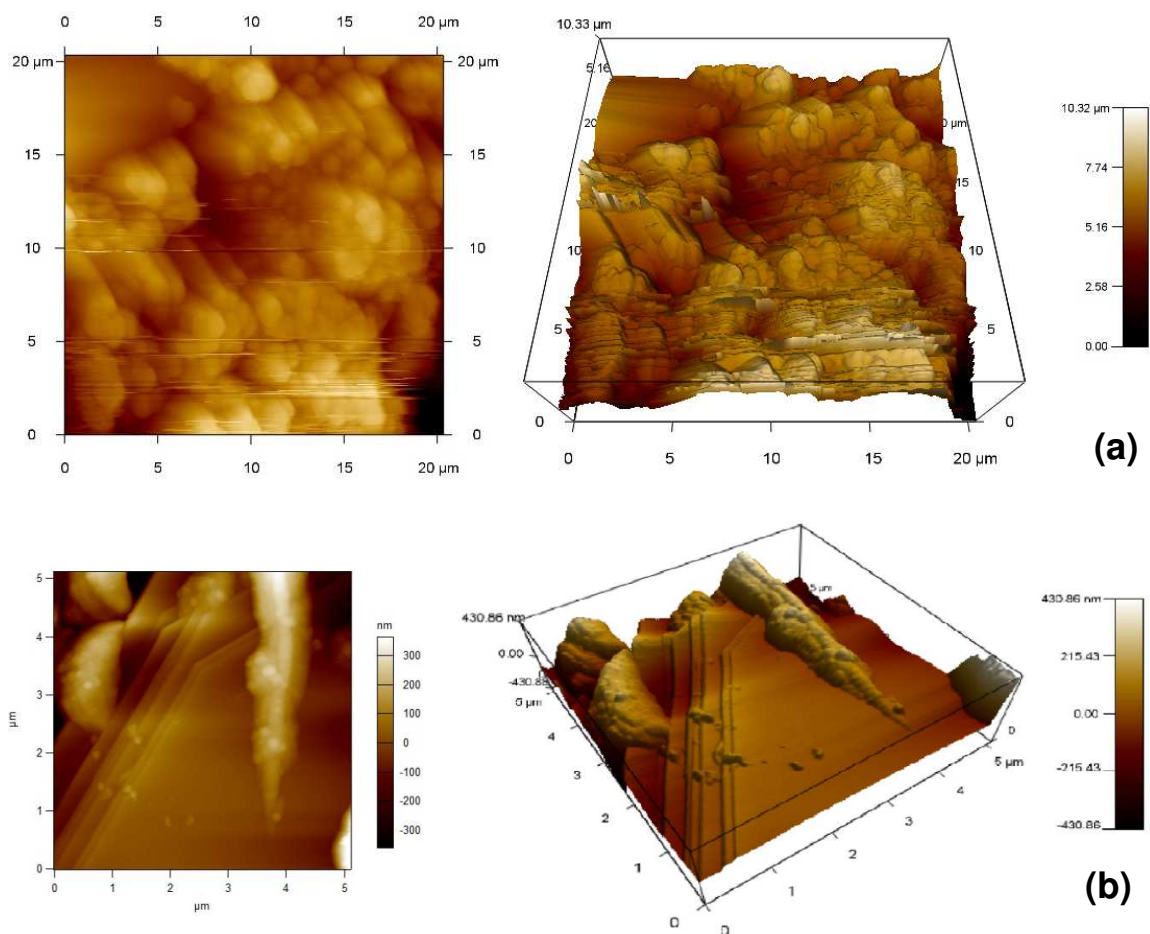


374



375

376 Figure 2. Electrochemical (left axis) and conductance (right axis) simultaneous study for
 377 the electropolymerization of (a) BTh and (b) BTh/MWCNT mixture in a ACN/LiClO₄ 0.1
 378 M, 0.015 M BTh, 40 mg MWCNT solution, $T = 25^{\circ}\text{C}$, $\nu = 0.02 \text{ V s}^{-1}$, WE=Pt IDMAE 10
 379 μm (1 cm x 0.5 cm), CE=Pt foil, $E_i = -0.70 \text{ V vs Ag/AgNO}_3$, $E_f = 1.20 \text{ V vs Ag/AgNO}_3$, 5
 380 cycles and $\Delta V = 10 \text{ mV}$.



381 Figure 3. AFM micrographs of (a) PBTh and (b) PBTh/MWCNT composite obtained in
 382 ACN/LiClO₄ 0.1 M, 0.015 M BTh, $T = 25^{\circ}\text{C}$, $\nu = 0.02 \text{ V s}^{-1}$, WE=Pt foil ($A = 0.48 \text{ cm}^2$),
 383 CE=Pt foil, $E_i = -0.70 \text{ V vs Ag/AgNO}_3$, $E_{\lambda}=1.2 \text{ V vs Ag/AgNO}_3$, 5 cycles. (b) same
 384 conditions as (a) but in the presence of 40 mg MWCNT.

385

